

CHROMOSPHERIC OBSERVATIONS IN THE HELIUM 1083NM LINE - A NEW INSTRUMENT

Neil Murphy⁽¹⁾, Edward Smith⁽¹⁾, Wayne Rodgers⁽²⁾, Stuart Jefferies⁽³⁾

⁽¹⁾*Jet Propulsion Laboratory, 4800 Oak Grove Drive, Pasadena, CA, USA, Neil.Murphy@jpl.nasa.gov, Edward.J.Smith@jpl.nasa.gov:*

⁽²⁾*Eddy Company, 13590 Niabi Road, Apple Valley, CA, USA, wayner@eddyco.com:*

⁽³⁾*Maui Scientific Research Center, University of New Mexico, Kihei, HI, USA, stuartj@msrc.unm.edu:*

ABSTRACT

Photometric, spectroscopic and polarimetric observations in the Helium 1083 nm line provide important diagnostic information on the structure and dynamics of the chromosphere. We describe an imaging instrument designed to probe the chromosphere in the Helium 1083nm line, based on a Helium magneto-optical filter. The instrument has two narrow passbands (≈ 0.006 nm) in the wings of each line of the Helium 1083nm triplet, high throughput and stability, making it ideal for making high cadence observations in support of studies of chromospheric dynamics and wave propagation. We describe the characteristics of the instrument and present preliminary observations and discuss future plans.

1. INTRODUCTION

The Helium 1083 nm line is widely used as a diagnostic of processes in the solar atmosphere. Helium 1083 nm emissions can be used to study the dynamics of chromospheric and coronal structures (outflows, filaments and dark points for example) and magnetic fields (*Lin et al., 1998, Lagg et al., 2004*). While it is formed in the chromosphere, it is also sensitive to processes in the photosphere and the overlying corona. For example, the presence of coronal holes can be inferred from Helium 1083nm images (e.g. *Harvey and Recely, 2002*), and CME-associated coronal EIT waves have been shown to be related to waves seen in chromospheric Helium 1083nm images (*Gilbert et al., 2004*).

Several types of instruments fill the need for Helium 1083nm observations, from traditional spectrometers (e.g. *Hofmann et al., 1995*) to filter based instruments (e.g. *Elmore et al., 1998*). The instrument we have developed is a filter-based imaging photometer, based on a magneto-optical filter (MOF). An MOF-based instrument can have several potentially useful features: narrow pass-bands (≈ 60 mÅ) that are insensitive to acceptance angle, simplifying optical design; pass-bands that can be stepped across the spectral line (*Isaak & Jones, 1988*) allowing measurements of equivalent width, independent calibration of Doppler shifts and measurements of vector magnetic fields; and high

throughput (in theory, up to 50%) allowing high cadence measurements to be made.

Ohman (*1956*) was the first to use magneto-optical filters for solar observations creating narrow band-pass birefringent filters at resonance lines of hydrogen, neon and sodium. Following this initial work, filters operating in the sodium 589 nm and potassium 770 nm lines were developed and have been used successfully both in solar physics and astronomy (e.g. *Cimino, et al., 1967, Cacciani and Fofi, 1979, Tomczyk et al. 1995, Isaac et al, 1989, Innis et al., 1991, 1994, Bedford et al., 1995, Cacciani et al, 1995*). In addition to their scientific use, MOF designs have been proposed for use as narrow passband, high background rejection filters in laser communication applications. For these MOF designs the goal was to match the filter transmission to laser wavelengths that are potentially useful for communications, leading to filter designs based on cesium (e.g. *Menders et al., 1992, Zhang et al., 1996*), rubidium (e.g. *Dick and Shay 1991*), calcium, strontium (*Gelbwachs and Chan, 1990*) and Thallium (*Oehry et al., 1991*). These filters involved both ground state transitions and also transitions from optically pumped excited levels.

In this paper we will describe a prototype instrument, designed to explore the properties of an MOF-based chromospheric photometer and present preliminary photometric observations.

2. A HELIUM MAGNETO-OPTICAL FILTER

The Helium 1083nm filter described here is similar in concept to those produced by Ohman for H and Ne: It is comprised of two crossed calcite polarizers surrounding a helium gas cell, which is immersed in a strong longitudinal magnetic field of 1-4 kG (Fig. 1a). In the absence of any optical activity in the helium cell, the crossed polarizers would block the transmission of light through the filter (with an extinction ratio of a few parts in 10^6), however, magneto-optical effects (circular birefringence and dichroism), caused by anomalous dispersion at wavelengths close to the helium absorption lines, modify the polarization state of the light passing through the cell. This change in polarization state means that light in these passbands can then pass through the second polarizer, producing an extremely

narrow band optical filter. A 10nm interference filter is used to block the residual light leaking through the polarizers and light from unwanted helium transitions.

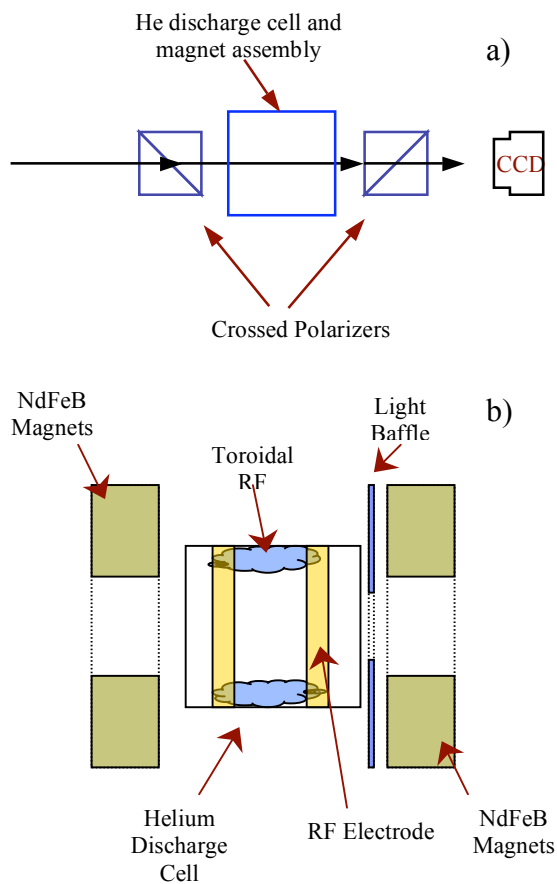


Figure 1 a) The overall layout of the test instrument showing the helium cell and magnet assembly placed between crossed polarizers. The arrows show the optical axis, which is parallel to the magnetic field. b) Details of the helium cell and magnet assembly, showing the placement of the magnets relative to the discharge cell.

The pass-band separation is determined by the magnetic field strength, the metastable helium column density in the cell and oscillator strength of the line.

The 1083 nm triplet is formed by the transition from the metastable 2^3S_1 state to the 2^3P state; therefore we must have a population of metastable Helium atoms within the cell for it to operate. To produce the metastable population, the helium is excited by a radio-frequency (RF) discharge. Upon recombination a small percentage of atoms return to the metastable 2^3S_1 state. The production rate of metastable helium atoms is determined by the RF electric field strength, frequency and the cell geometry.

2.1. Filter Construction

There are two basic magnetic field geometries used in constructing magneto-optical filters – the magnetic field can be parallel to the optical axis of the filter or it can be perpendicular to the optical axis and inclined at 45° to the crossed polarizers. Both geometries have

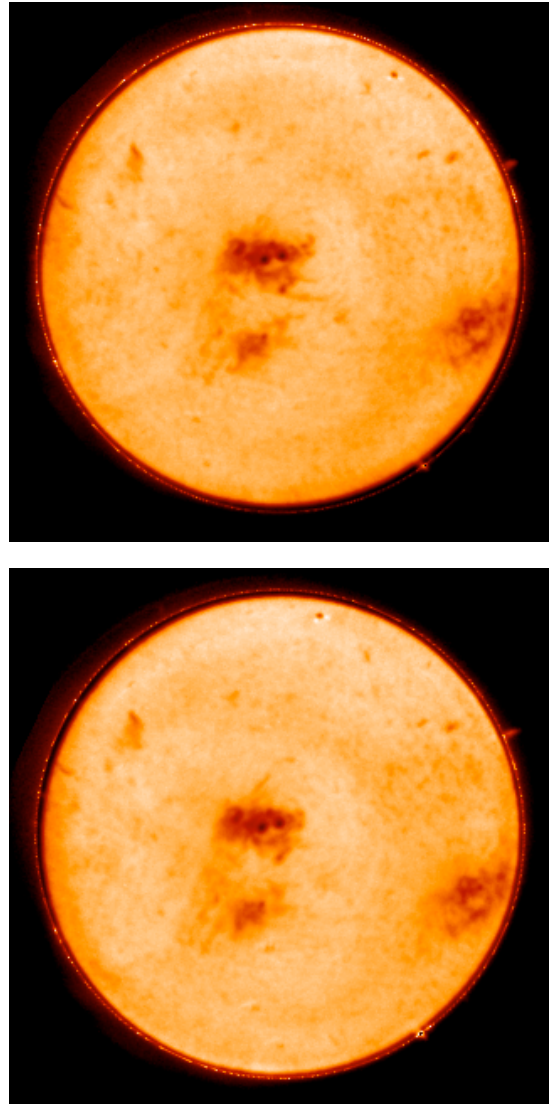


Figure 2. Two images taken using the Helium 1083nm MOF. The images were taken approximately 2 hours apart on July 22nd 2004.

advantages, depending on the filter application, but in the case of the Helium MOF we have chosen the latter, more common geometry. One particular advantage of this choice is that it simplifies the creation of an RF discharge with the desired properties.

The use of an RF discharge creates the required metastable Helium population, however, it also produces both line and continuum optical emission. To

produce an effective solar observing instrument we must prevent emission from the discharge from contaminating the resulting solar image. The discharge is produced by coupling an RF source (at frequencies between 18 and 30 MHz) to electrodes attached to the outside of the cylindrical cell. These electrodes are arranged in bands around the cell, which, together with the chosen magnetic field geometry, produces a toroidal discharge close to the cell wall. The instrument is arranged such that the optical path is centered on the toroid (Fig. 1b). Metastable helium atoms created in the discharge then diffuse through the helium to the center of the cell. The resulting metastable atom density is determined by the balance between the production rate close to the cell walls and various loss mechanisms, which are dominated by collisions with other helium atoms and with the cell walls. With the above filter geometry, and appropriate baffling, the photon flux reaching the CCD from the discharge is less than 2% of the flux from the sun.

3. PRELIMINARY OBSERVATIONS

To verify the instrument concept and provide data to help refine its design, we have performed test measurements using the single-stage Helium MOF. The primary purpose of these tests was to determine the filter throughput as a function of discharge power, cell volume, shape, electrode position and Helium pressure. The instrument used to make the test images shown here used a 40mm long 40mm diameter cell filled with pure helium at a pressure of 120 Pa, with a longitudinal magnetic field of 2kG. Light was fed to the instrument from a heliostat with a 50mm objective potentially allowing an image resolution of ≈ 5 arcsec, although the actual performance is seeing-limited to > 10 arcsec.

Fig. 2 shows two images taken approximately 2 hours apart on July 22nd 2004 (during this period, the instrument was operated at a cadence of one image every 35s). After dark frame subtraction and flat fielding the images were divided by an empirical limb-darkening function. Subtle brightness variations on the disk are in part due to flat-fielding errors and scattered light. Off-limb brightness is enhanced to show prominences, which can clearly be seen off the western limb in each image. In Fig. 2 we can see numerous absorption features, typical of chromospheric images in the 1083nm helium line, some of which have contrasts over 25%. A large active region dominates the center of the disk in each image and is centered on two sunspots. Evolution of the filaments on the southern edge of this active region can be seen between the two images.

4. FUTURE PLANS

The filter described above is the first stage in the development of a MOF-based helium 1083nm Doppler-magnetograph. To provide Doppler sensitivity, a

second filter stage is required that can discriminate between passbands on either side of the selected absorption line (usually referred to as the wing selector, *Cacciani and Fofi, 1979*). The use of a wing selector allows images in each passband to be made simultaneously (*Tomczyk et al. 1995*), which is critical for the production of low-noise data. The normalized difference of these images produces an image proportional to line-of-sight velocity, i.e. a Dopplergram. The constant of proportionality relating these Dopplergrams to actual line-of-sight velocity needs to be determined by calibration. Because the shape of the Helium 1083nm line varies significantly as a function of time and position on the solar disk, this

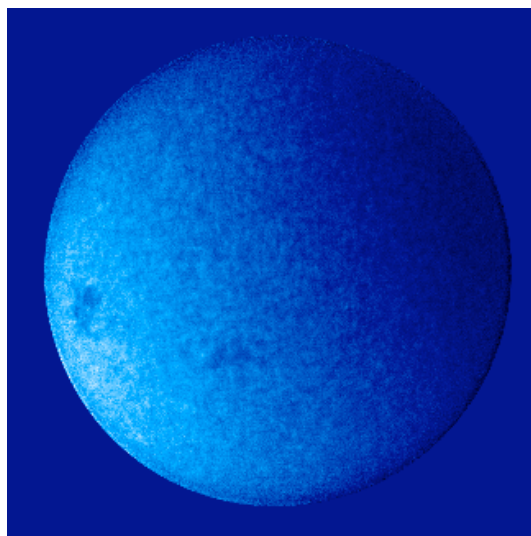


Figure 3. A Doppler image produced by a Calcium 422.7nm magneto-optical filter. The Calcium 422.7 MOF, together with the He 1083nm MOF will form part of the MOTH II experiment.

calibration will be performed by stepping the instrument passbands between successive images using a variable magnetic field (*Isaak & Jones, 1988*). In this way, the line slope at the wavelength of each passband can be recovered from the data. Adding a polarimetric capability to the instrument to determine Stokes V as well as intensity will allow the measurement of longitudinal magnetic fields.

The first scientific use of the Helium MOF will be as part of the MOTH II experiment that will ultimately be deployed to the South Pole. MOTH II will make Doppler and magnetic measurements in the solar atmosphere simultaneously at four different heights, and from these data identify the different types of magneto-acoustic waves present. To provide high signal-to-noise data, observations will be made from the geographic South Pole where the Sun can typically be observed without interruption for periods of twenty days or more.

MOTH II will have four channels covering the Ca 422.7nm, Na 589nm K 770nm and Helium 1083nm spectral lines, allowing sampling of the solar atmosphere from the photosphere to the high chromosphere. While Na 589nm and K 770nm MOFs have been used widely, both the Helium 1083nm and Ca 422.7nm MOFs are new developments. As an example of the other data types that will be collected by the MOTH II experiment, Fig. 3 shows a Dopplergram taken using a Ca 422.7 MOF. The rotational velocity of the sun is clear in the Dopplergram and the solar velocity field is clearly seen superimposed on the rotation.

In order to be sensitive to waves propagating above the acoustic cutoff frequency, the MOTH II experiment will collect Doppler and line-of-sight magnetic field images in all four channels with a 10s cadence. Full-disk images will be produced with a spatial resolution of 4 arcsec and the instrument will have a high-resolution mode with 1 arcsec spatial resolution.

5. ACKNOWLEDGEMENTS

Results presented here represent one aspect of research done by the Jet Propulsion Laboratory, California Institute of Technology, under contract to the National Aeronautics and Space Administration. The Ca MOF was developed at the Eddy Co, using internal R&D funding.

6. REFERENCES

- Bedford, D.K., W.J. Chaplin, D.W. Coates, A.R. Davies, J.L. Innes, G.R. Isaak and C.C. Speake, *Mon. Not. R. astr. Soc.*, **273**, 367, 1995a.
- Bedford, D.K., W.J. Chaplin, A.R. Davies, J.L. Innes, G.R. Isaak and C.C. Speake, *Mon. Not. R. astr. Soc.*, **269**, 435, 1994.
- Bedford, D.K., W.J. Chaplin, A.R. Davies, J.L. Innes, G.R. Isaak and C.C. Speake, *Astron. Astrophys*, **293**, 377, 1995b.
- Boumier, P., H.B. van der Raay and T. Roca Cortes, *Astron. Astrophys. Suppl. Ser.*, **107**, 177, 1994.
- Cacciani, A and M. Fofi, *Solar Physics*, **50**, 179, 1979.
- Cacciani, A., P.F. Moretti, M Dolci, E. Brocato, E.J. Smith, *Geophys. Res. Lett.*, **22**, 17, 2437-2440, 1995.
- Cimino, M., A. Cacciani and N. Sopranzi, *Solar Physics*, **3**, 618, 1967.
- Dick, D. J., Shay, T. M., Ultrahigh-noise rejection optical filter, *Opt Lett*, **16**, 11, 867-869, 1991.
- Elmore, D.F., G.L. Card, C.W. Chambellan, D.M. Hassler, H.L. Hull, A.R. Lecinski, R.M. MacQueen, K.V. Streander, J.L., Streete and O.R. White, Chromospheric helium imaging photometer, *Applied Optics*, **37**, No 19, 1998.
- Gelbwachs, J. A., Chan, Y. C., Lasers '91; Proceedings of the 14th International Conference on Lasers and Application, 649-656. 1991.
- Gilbert, Holly R.; Holzer, Thomas E.; Thompson, Barbara J.; Burkepile, Joan T., *ApJ*, **607**, pp. 540-553, 2004.
- Harvey, Karen L.; Recely, Frank, *Solar Physics*, v. **211**, Issue 1, p. 31-52 (2002).
- Hoffman, J., F-L. Deubner, B. Fleck, GONG'94 ASP Conf. series Vol 76, Eds. Ulrich, R.K., and E.J. Rhodes, 1995.
- Innes, J.L., G.R. Isaak, C.C. Speake, R.I. Brazier and H.K. Williams, *Mon. Not. R. astr. Soc.*, **249**, 643, 1991.
- Innes, J.L., G.R. Isaak, C.C. Speake, W.J. Chaplin, R.I. Brazier, and A.R. Jones, *Mon. Not. R. astr. Soc.*, **271**, 573, 1994.
- Isaak, G.R., A.R. Jones, *Adv. helio- and astroseismology: I.A.U.symp.* **123** p.4671, 1988
- Isaak, G.R., C.P. McLeod, H.B. Van der Raay, P.L. Pallé, and T. Roca Cortés, *Astron. Astrophys*, **208**, 289, 1989
- Jefferies, S.M. , J. D. Armstrong, A. Cacciani, Cynthia Giebink, N Murphy and W Rodgers, abstract #SH13C-12 AGU, Spring 2005
- Lagg, A.; Woch, J.; Krupp, N.; Solanki, S. K., Retrieval of the full magnetic vector with the He I multiplet at 1083 nm. Maps of an emerging flux region, *A&A*, v.**414**, p.1109-1120, 2004.
- Lin, Haosheng; Penn, Matt J.; Kuhn, Jeffrey R., Hel 10830 Angstrom Line Polarimetry: A New Tool to Probe the Filament Magnetic Fields, *Astrophysical Journal* v.**493**, p.978, 1998.
- Menders, J., Searcy, P. A., Roff, K., Korevaar, E., Blue cesium Faraday and Voigt magneto-optic atomic line filters, *Opt Lett*, **17**, 19, 1388-1390, 1992.
- Morgan-Vandome, S.C. Ph.D. thesis, School of Physics and Space Research, University of Birmingham, 1991.
- Oehry, B P., Schupita, W., Magerl, G., Lamp-pumped thallium atomic line filter at 535.046 nm, *Opt Lett*, **16**, 1620-1622, 1991.
- Ohman, Y. *The Observatory*, **79**, 89, 1956 and *Stockholms Observatoriums Annaler*. **19**. No. 4, 1956
- Rodgers, W, N. Murphy, S. M. Jeffries, A Calcium-Based Magneto-Optical Filter, AGU, Abstract #SH13C-13 Spring 2005
- Tomczyk, S., K. Streander, G. Card, D. Elmore, H. Hull, and A. Cacciani, An Instrument to Observe Low-Degree Solar Oscillations, *Solar Physics*, **159**, 1, 1995.
- Zhang, Y., Bi, Y., Jiang, X., Yu, J., Ma, Z., Magneto-optical dispersion filter at the Cs 455,459-nm transition, Proc. SPIE **2893**, 120-123, Kam T. C., Shui-sheng J., Franklin K. T., Eds., 1996.